JACS
JOURNAL OF THE AMERICAN CHEMICAL SOCIETY

Article

pubs.acs.org/JACS

Characterization of the DNA-Mediated Oxidation of Dps, A Bacterial Ferritin

Anna R. Arnold, Andy Zhou, and Jacqueline K. Barton*

Division of Chemistry and Chemical Engineering, California Institute of Technology, Pasadena, California 91125, United States

Supporting Information

ABSTRACT: Dps proteins are bacterial ferritins that protect DNA from oxidative stress and have been implicated in bacterial survival and virulence. In addition to direct oxidation of the Dps iron sites by diffusing oxidants, oxidation from a distance via DNA charge transport (CT), where electrons and electron holes are rapidly transported through the base-pair π-stack, could represent an efficient DNA protection mechanism utilized by Dps. Here, we spectroscopically characterize the DNA-mediated oxidation of ferrous iron-loaded Dps. X-band EPR was used to monitor the oxidation of DNA-bound Dps after DNA photooxidation using an intercalating ruthenium photooxidant and the flash-quench technique. Upon irradiation with poly(dGdC)$_2$, a signal arises with g = 4.3, consistent with the formation of mononuclear high-spin Fe(III) sites of low symmetry, the expected oxidation product of Dps with one iron bound at each ferroxidase site. When poly(dGdC)$_2$ is substituted with poly(dAdT)$_2$, the yield of Dps oxidation is decreased significantly, consistent with guanine radical intermediates facilitating Dps oxidation. We have also explored possible protein electron transfer (ET) intermediates in the DNA-mediated oxidation of ferrous iron-loaded Dps. Dps proteins contain a conserved tryptophan residue in close proximity to the iron-binding ferroxidase site (W52 in *E. coli* Dps). In EPR studies of the oxidation of ferrous iron-loaded Dps following DNA photooxidation, a W52A Dps mutant was significantly deficient compared to WT Dps in forming the characteristic EPR signal at g = 4.3, consistent with W52 acting as an ET hopping intermediate. This effect is mirrored in vivo in *E. coli* survival in response to hydrogen peroxide, where mutation of W52 leads to decreased survival under oxidative stress.

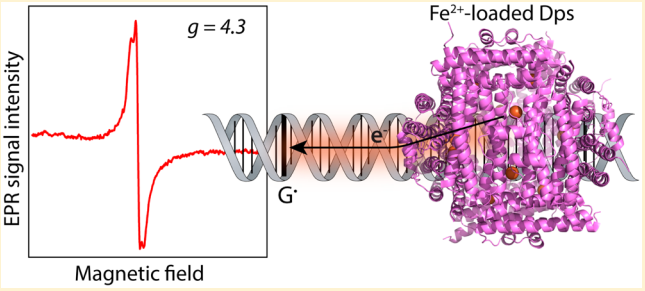

INTRODUCTION

Dps proteins are dodecameric (12-mer) bacterial ferritins that protect DNA from oxidative stress, and have been implicated in bacterial survival and virulence.[1] This protection is thought to derive from the ferroxidase activity of Dps, where Dps proteins simultaneously deplete ferrous iron and hydrogen peroxide, reactive species that can otherwise form damaging hydroxyl radicals via Fenton chemistry.[2] Like other ferritins, Dps proteins are spherical, with a hollow core where oxidized iron is reversibly stored. Some Dps proteins nonspecifically bind DNA, such as that from *Escherichia coli* which utilizes N-terminal lysine residues for DNA binding.[3] Within cells, Dps is upregulated by the transcriptional regulator OxyR in response to oxidative stress;[4] Dps is also upregulated in stationary phase, when an additional physical component of Dps protection may be biocrystallization with DNA.[5]

DNA charge transport (CT), where electrons and electron holes are efficiently transported through the base-pair π-stack, represents a powerful means to carry out redox chemistry from a distance.[6] Moreover, DNA CT chemistry is remarkably sensitive to the integrity of the intervening DNA. We have explored biological applications of DNA CT, where we have seen this chemistry being utilized as a first step for DNA repair proteins containing 4Fe4S clusters to signal one another and thus localize to the vicinity of a lesion within the vast milieu of the genome.[7] We have also found examples where DNA CT facilitates the selective activation of redox-active transcription factors to respond to oxidative stress from a distance.[6] Given these applications of DNA CT, we considered whether Dps, in addition to interacting directly with diffusing oxidants, might also utilize DNA CT to protect DNA from a distance. Guanine is the most easily oxidized base within DNA, and the presence of adjacent stacked guanines further lowers the 5′-guanine oxidation potential;[8] thus, radicals are characteristically formed at guanine multiplets upon DNA photooxidation.[9] A long distance protection mechanism via DNA CT would involve electron transfer from Dps through the DNA π-stack to fill the hole on guanine radicals, restoring the integrity of the DNA. In this way, Dps could respond to an oxidative affront to the DNA, even if the protein is bound, at the minimum, a hundred base-pairs away.[10]

Indeed, we have previously shown biochemically that *E. coli* Dps loaded with ferrous iron at the ferroxidase sites can protect DNA from oxidative damage through DNA CT.[11] [Ru(phen)(dppz)(bpy′)]$^{2+}$, where phen is 1,10-phenanthroline, dppz is

Received: June 23, 2016
Published: August 29, 2016

DOI: 10.1021/jacs.6b06507
J. Am. Chem. Soc. 2016, 138, 11290−11298

dipyrido[2,3-a:2′,3′-c]phenazine, and bpy′ is 4-butyric acid-4′-methyl-2,2′-bipyridine, was covalently tethered to the 5′ end of mixed-sequence 70-mer DNA and served as the distally tethered, intercalated photooxidant generated in situ by the flash-quench technique. Upon excitation with visible light ("flash"), the ruthenium(II) excited state can be oxidatively quenched ("quench") by a diffusing quencher, here $[Co(NH_3)_5Cl]^{2+}$, to form a highly oxidizing intercalated Ru(III) complex (1.6 V versus NHE).[12] In the absence of protein, oxidative damage is observed preferentially at a guanine triplet within the 70-mer DNA duplex. Titrating in ferrous iron-loaded Dps significantly attenuates the level of oxidative damage at the guanine triplet, while Apo-Dps and ferric iron-loaded Dps, which lack available reducing equivalents, do not display this protection.[11] Luminescence experiments rule out direct interaction between the ruthenium photooxidant excited state and Dps, consistent with a long-range DNA-mediated oxidation mechanism. Long-distance, DNA-mediated oxidation of Dps could be an effective mechanism for bacteria to protect their genomes from oxidative insults, contributing to pathogenic survival and virulence.

Here we spectroscopically characterize the DNA-mediated oxidation of ferrous iron-loaded Dps. Electron paramagnetic resonance (EPR) spectroscopy has previously been used to observe oxidation of the 4Fe4S cluster of the base excision repair glycosylase MutY following flash-quench DNA photooxidation.[12b] In this work, we use X-band EPR spectroscopy to observe the oxidation of DNA-bound *E. coli* Dps loaded with ferrous iron at the ferroxidase sites and to investigate the DNA-mediated characteristics of this oxidation (Figure 1).

We also explore possible protein electron transfer intermediates in the DNA-mediated oxidation of ferrous iron-loaded Dps. There is a highly conserved tryptophan residue in close proximity (approximately 5 Å) to the di-iron ferroxidase site in Dps proteins, W52 in *E. coli*.[13] Aromatic amino acids such as tryptophan and tyrosine can act as electron transfer (ET) hopping intermediates in proteins, allowing for rapid ET across the protein where a single ET process would be kinetically difficult.[14] Because of the location of this aromatic tryptophan residue between the ferroxidase site and the outer protein shell where the DNA must be located, it is an attractive candidate as a hopping intermediate to facilitate ET between the ferroxidase site of Dps and DNA. Previous work has suggested an important role for this conserved tryptophan residue in Dps proteins. Upon oxidation with hydrogen peroxide of Dps loaded with only 6 Fe(II)/Dps, UV−visible stopped flow experiments with *E. coli* Dps were able to observe spectra with maxima at 512 and 536 nm, consistent with a neutral tryptophan radical.[15] By comparison with site-directed mutagenesis studies on *L. innocua* Dps, which also contains a tyrosine residue nearby the ferroxidase site, the tryptophan radical in *E. coli* was ascribed to W52.[15] A double mutant of *L. innocua* Dps, where both of the aromatic residues in proximity to the ferroxidase site were mutated, was assayed for its ability to protect plasmid DNA from degradation by ferrous iron and hydrogen peroxide. Given that the protective capacity of the *L. innocua* Dps double mutant was significantly attenuated, it was concluded that these conserved aromatic residues act as a trap for electron holes generated by the oxidation of insufficient ferrous iron by hydrogen peroxide.[15,16] Interestingly, 24-mer ferritins contain a conserved tyrosine residue in close proximity to the ferroxidase site that has also been proposed to act as a molecular capacitor, although other studies contend with this hypothesis.[17] Overall, the conserved aromatic residue in close proximity to the ferroxidase site may play an important role in ferritins.

Thus, here we investigate two *E. coli* Dps W52 mutants: W52Y, where an aromatic residue is maintained at this position, and W52A, which abolishes the aromatic residue adjacent to the ferroxidase site. We compare these mutants with the wild-type (WT) protein in EPR studies of the oxidation of ferrous iron-loaded Dps following DNA photooxidation. Because the intercalating ruthenium photooxidant is a one-electron oxidant, sending one electron hole at a time into the DNA π-stack, we examine the possible role of *E. coli* Dps W52 as an electron transfer hopping intermediate rather than a molecular capacitor. In addition to EPR, we also probe the role of W52 with respect to cellular survival in studies of *E. coli* under oxidative stress.

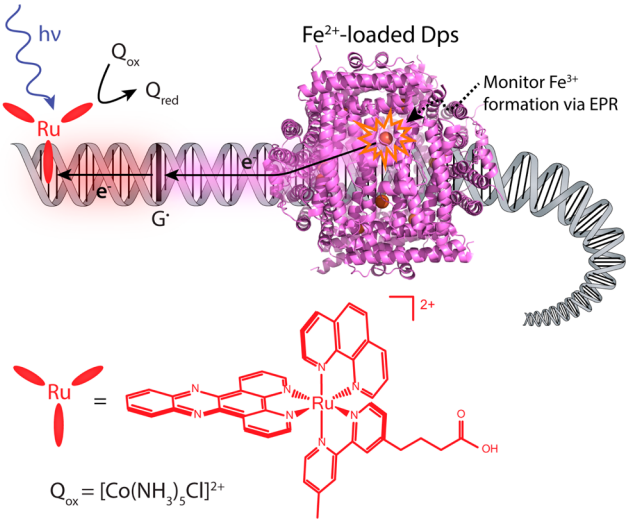

Figure 1. Schematic depicting DNA-mediated oxidation of ferrous iron-loaded Dps to fill the guanine radical hole generated by flash-quench chemistry. Visible light first excites an intercalated non-covalently bound ruthenium(II) photooxidant ($[Ru(phen)(dppz)(bpy')]^{2+}$, which is then oxidatively quenched by a diffusing quencher (Q, $[Co(NH_3)_5Cl]^{2+}$). This highly oxidizing Ru(III) species abstracts an electron from DNA, preferentially forming guanine radicals. The goal of this study is to observe DNA-mediated electron transfer from the ferrous iron bound at the ferroxidase sites in Dps to the guanine radical by monitoring the appearance of oxidized iron products via EPR. *E. coli* Dps PDB: 1dps.

EXPERIMENTAL SECTION

Materials. The alternating copolymer DNA duplexes $poly(dGdC)_2$ and $poly(dAdT)_2$ were purchased from Sigma. The DNA duplexes were passed through Biorad spin columns (6 K MWCO) before use and quantified based on their molar absorptivity values in base-pairs,[18] ($poly(dGdC)_2$: ε_{254} = 16 800 $M^{-1}cm^{-1}$, $poly(dAdT)_2$: ε_{262} = 13 200 M^{-1} cm^{-1}). Duplexes were then dried on a speed-vac, brought into an anaerobic chamber, and resuspended in deoxygenated buffer for EPR experiments. Buffers (50 mM Tris or 50 mM MOPS, pH 7.0, 150 mM NaCl, 5% glycerol) were deoxygenated in a Schlenk flask by at least 4 cycles of freeze−pump−thaw.

$[Ru(phen)(dppz)(bpy')]^{2+}$ was synthesized according to published methods,[19] purified by reversed-phase chromatography, and characterized by NMR and ESI mass spectrometry (expected for the +2 ion: 409.62 m/z, observed: 410.2 m/z). The ruthenium photooxidant was brought into the anaerobic chamber as a solid powder, resuspended with deoxygenated buffer, and a sample removed for quantification based on UV−vis absorption (ε_{440} = 21 000 M^{-1}

DOI: 10.1021/jacs.6b06507
J. Am. Chem. Soc. 2016, 138, 11290−11298

cm^{-1}). $[Co(NH_3)_5Cl]Cl_2$ was purchased from Sigma (99.995% pure) and used as received. The Co quencher was brought into the anaerobic chamber as a solid powder, resuspended with deoxygenated buffer, and a sample removed for quantification based on UV−vis (ε_{550} = 47.5 M^{-1} cm^{-1}).

W52 Mutagenesis. The W52A and W52Y *E. coli* Dps mutants were made with a Quikchange II-E Site-Directed Mutagenesis Kit (Stratagene) using a pBAD18-*dps* plasmid (containing the WT *E. coli dps* gene and an ampicillin resistance cassette) donated by Dr. Roberto Kolter as a template.[20] Primers were purchased from Integrated DNA Technologies. All mutagenized plasmids were sequenced (Laragen) to confirm the desired sequences. After creating the mutant pBAD18-*dps* plasmids, the *E. coli* cell line ZK2471 (*dps*::*kan* Δ*recA* Δ*ara*) donated by Dr. Roberto Kolter was made electrocompetent and the plasmid was transformed via electroporation into these cells. Primer sequences are provided in the Supporting Information (SI).

Dps Overexpression, Purification, and Iron Loading. WT and W52 mutant *E. coli* Dps proteins were overexpressed and purified according to previous procedures,[11] with one significant modification: the addition of a HiTrap Heparin HP affinity column to ensure removal of endogenous DNA. A detailed protocol is provided in the SI. Proteins were deoxygenated in Schlenk tubes by rapid cycles of vacuum and argon according to previous procedures[11] and brought into the anaerobic chamber. Proteins were then anaerobically incubated with excess ferrous iron to load the ferroxidase sites, with unbound iron removed by size exclusion chromatography.[11] The number of iron ions bound per Dps dodecamer was then quantified by separately measuring the protein and iron concentration. Protein concentrations were measured using either a Bradford assay (Sigma) or ε_{280} values calculated using the ExPASy ProtPram tool (http://web.expasy.org/-protparam/) with calculated molar absorptivity values for WT, W52A, and W52Y *E. coli* Dps dodecamers of 1.86 x10^5 $M^{-1}cm^{-1}$, 1.20 × 10^5 $M^{-1}cm^{-1}$, and 1.37 × 10^5 $M^{-1}cm^{-1}$, respectively. Iron concentration was quantified according to $[Fe(bpy)_3]^{2+}$ absorbance (ε_{522} = 8790 $M^{-1}cm^{-1}$) using a denaturing method detailed elsewhere.[11] As-purified, Dps was considered to be Apo-Dps with typically ≤1 Fe/Dps.

Circular Dichroism of Dps. Protein concentrations were determined using the calculated ε_{280} values described above. Spectra were recorded at 25 °C on a Model 430 circular dichroism spectrometer (AVIV) in a buffer consisting of 50 mM Tris, pH 7.0, 150 mM NaCl. The spectra shown are the average of three individual scans, with a spectrum of buffer alone subtracted.

EPR Sample Preparation. EPR samples were prepared in an anaerobic chamber using the anaerobic materials outlined above. Samples were loaded into EPR tubes within the anaerobic chamber, sealed with septa, and parafilmed around the septa seal. Under the conditions used in these experiments, all samples containing both Dps and DNA precipitated, expected behavior associated with Dps condensing DNA. EPR tubes were then brought out of the anaerobic chamber, frozen in liquid nitrogen, and kept in the dark until measurement. Precipitated samples were thoroughly mixed before freezing in liquid nitrogen. For chemically oxidized samples, ferrous iron-loaded protein (approximately 120 μL) was added to the bottom of an EPR tube. Approximately 20 μL of ferricyanide solution was added to the top of the EPR tube, which was then sealed. Upon removal from the anaerobic chamber, the solutions were mixed together and immediately frozen in liquid nitrogen within approximately 5−10 s of the initiation of mixing.

EPR Experiments. EPR spectra were measured on an X-band Bruker EMX spectrometer equipped with an ER4119HS resonator and an Oxford ES9000 cryostat. Instrumental settings are detailed in figure captions, but were generally as follows: modulation amplitude = 10 G at 100 kHz, frequency = 9.37 GHz, microwave power = 6.4 mW, and temperature = 10 K. Samples in Suprasil quartz EPR tubes were irradiated while freezing in liquid nitrogen in an unsilvered Dewar. The excitation source was a xenon lamp equipped with a lens to focus the beam and a 320 nm long-pass filter to remove UV light. Each sample was irradiated for approximately 10 s. For each sample, a dark control (DC) EPR spectrum was first measured at 10 K. The sample was then thawed, mixed, and irradiated while freezing with liquid nitrogen as described. The EPR spectrum of the irradiated sample was then measured under identical instrumental settings. For data analysis, the DC spectrum was smoothed and subtracted from the irradiated sample.

Hydrogen Peroxide Survival Experiments. This protocol is adapted from that reported by Martinez and Kolter.[20] Hydrogen peroxide was purchased from Macron (30% solution). Lyophilized catalase from bovine liver (≥20 000 units/mg protein) was purchased from Sigma and resuspended in buffer (50 mM K_3PO_4, pH 7) to make a stock concentration of 0.4 mg/mL. Overnight cultures of the *E. coli* ZK2471 strain (*dps*::*kan* Δ*recA* Δ*ara*) containing WT, W52A, or W52Y pBAD18-*dps* plasmids were prepared by inoculating single colonies in 5 mL of LB media containing 100 μg/mL ampicillin and 50 μg/mL kanamycin. After overnight shaking at 37 °C, the cultures were diluted 1:500 into 10 mL of fresh LB media also containing antibiotics. For each WT, W52A, and W52Y, both induced and uninduced 10 mL cultures were prepared: L-arabinose was added to induce Dps overexpression (0.2% w/v final concentration), and an equivalent volume of sterile water was added to uninduced cells. Cultures were then incubated at 37 °C with shaking (200 rpm) for 3 h until OD_{600} = 0.3−0.4 (exponential phase). Separately, the growth of the induced cultures were monitored over 8 h for growth differences. Once reaching exponential phase, cultures were serially diluted in LB media for a total of 10 000-fold dilution with a final 1 mL aliquot volume. Hydrogen peroxide was added to these aliquots to attain a final concentrations of 3 or 5 mM in the cell aliquots and mixed by pipetting. After 15 min at RT, catalase solution was added to each aliquot to stop the reaction (50 μL, working concentration: 50 μg/mL culture) and mixed by pipetting. Cultures were incubated for 15 min after catalase addition to ensure complete hydrogen peroxide reaction. Finally, cultures were plated in 10 μL droplets onto LB agar plates containing ampicillin and kanamycin and incubated at 37 °C overnight. The number of colonies in each droplet was manually counted the subsequent day after plate imaging.

RESULTS

EPR Spectroscopy of WT *E. coli* Dps. In spectroscopic studies with Dps, we expect to observe the oxidation of mononuclear iron sites under the conditions of this study. At the intersubunit ferroxidase sites of Dps, two irons are bound by two conserved histidine ligands and two conserved carboxylate ligands, glutamate and aspartate.[1] This ligand coordination sphere creates two binding sites with very different iron affinities: while one site has a relatively high affinity, the other site binds iron weakly.[21] After binding, ferrous iron is oxidized and shuttled to the core of the protein for storage. Whereas 24-mer ferritins react rapidly with dioxygen as an oxidant, Dps proteins react slowly with dioxygen and much more quickly with hydrogen peroxide.[2] We have previously found that ferricyanide also functions well as a chemical oxidant of *E. coli* Dps in solution.[11] Whereas full occupation of the 12 di-iron centers of the protein would correspond to 24 Fe(II)/Dps, we have found that under the anaerobic conditions used in our experiments (i.e., in the absence of oxidants), *E. coli* Dps binds only 12 Fe(II)/Dps.[11,22] This loading agrees with studies on *Bacillus anthracis* and *Listeria innocua* Dps proteins, where a bridging oxidant seems to be required to tether the lower affinity iron and form the di-iron site.[21,23] Coupled with the specificity of iron binding evidenced by its abrogation in the *E. coli* Dps ferroxidase site double mutant H51G/H63G, the 12 Fe(II)/Dps corresponds to binding only at the higher affinity iron site of each ferroxidase center in the dodecameric protein.

Mononuclear high-spin Fe(III) sites of low symmetry (i.e., nonheme) typically display an EPR signal with an apparent *g*-

DOI: 10.1021/jacs.6b06507
J. Am. Chem. Soc. 2016, 138, 11290−11298

value of 4.3, and this is what we observe (Figure 2).[24,25] This mononuclear high-spin Fe(III) signal at g = 4.3 has been frequently reported in the EPR spectra of 24-mer ferritins.[26] The EPR spectrum of iron-bound Dps proteins is consistent but has been reported only once previously,[27] and has not yet been reported for *E. coli* Dps.

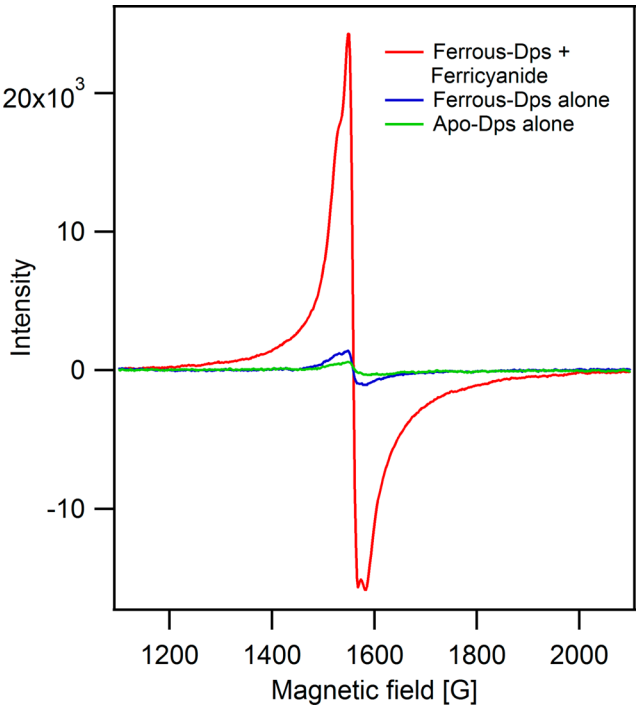

Figure 2. Chemical oxidation of WT *E. coli* Dps containing 12 Fe(II)/Dps with stoichiometric ferricyanide. Conditions: Dps concentration: 20 μM; Fe/Dps: 11.9 ± 0.2; Buffer: 50 mM Tris, pH 7, 150 mM NaCl, 5% glycerol. Instrument settings: modulation amplitude = 10 G at 100 kHz; frequency = 9.373 GHz; microwave power = 6.4 mW; and temperature = 10 K.

We first used chemical oxidation to examine the Dps oxidation products we might expect in DNA flash-quench studies. All EPR samples described in this study were prepared anaerobically in order to prevent dioxygen oxidation of ferrous iron loaded Dps. As expected, Apo-Dps, which has not been loaded with iron, and Dps loaded with ferrous iron are EPR-silent (Figure 2). However, when WT *E. coli* Dps loaded with 12 Fe(II)/Dps is mixed anaerobically with stoichiometric ferricyanide and frozen in liquid nitrogen, within 5−10 s, a split signal at g = 4.3 is observed at low temperature (10 K). Given that ferricyanide has a different g-value and ferrocyanide is EPR-silent, and that the steady-state UV−visible spectrum of ferrous iron-loaded Dps incubated with ferricyanide indicates the formation of oxidized iron species,[11] this signal at g = 4.3 can be assigned to oxidized ferric iron at the mononuclear ferroxidase site in Dps. This signal was confirmed to be neither power saturated nor overmodulated under the conditions used in this study. No other EPR-active species are apparent in wide spectra from 500 to 4500 gauss (data not shown). When instead the ferrous iron-loaded Dps was incubated with ferricyanide for much longer times, no EPR-active species were observed (data not shown), likely because the oxidized iron was translocated to the core of the protein, forming EPR-silent polynuclear species.

Next, we investigated the oxidation of DNA-bound WT Dps following DNA photooxidation via the flash-quench technique. We compare the yield of Dps oxidation with the alternating copolymers poly(dGdC)$_2$ and poly(dAdT)$_2$ in order to determine if guanine radical is an important intermediate in Dps oxidation. Here, the sample is irradiated in an EPR tube while freezing in liquid nitrogen in a clear dewar in order to trap reactive intermediates. For each sample, an individual dark control (DC) was measured at low temperature (10 K). The sample was then thawed, mixed, and irradiated while freezing to generate oxidative DNA damage via the flash-quench technique. Efforts were made to irradiate all samples under identical conditions for 10 s. The EPR spectrum of the irradiated sample was then remeasured under identical instrument settings. All spectra shown in Figure 3 have had an individual DC subtracted; thus, all features are a function of irradiation.

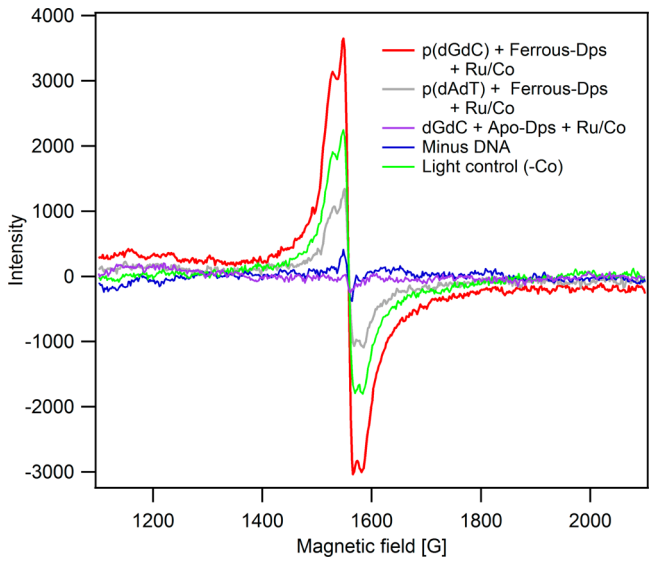

Figure 3. DNA-bound WT *E. coli* Dps oxidation via the flash-quench technique. All spectra have had an individual unirradiated spectrum subtracted; thus all features are a function of irradiation. Concentrations: 20 μM Dps (Fe(II)/Dps: 11.9 ± 0.2), 1 mM base-pairs poly(dGdC)$_2$ or poly(dAdT)$_2$ DNA, 20 μM [Ru(phen) (dppz) (bpy′)]$^{2+}$, 120 μM [Co(NH$_3$)$_5$Cl]$^{2+}$. Buffer: 50 mM Tris, pH 7.0, 150 mM NaCl, 5% glycerol. Minus DNA sample contains ferrous iron-loaded Dps, Ru, and Co, but lacks DNA; Light control contains ferrous iron-loaded Dps, poly(dGdC)$_2$ DNA, and Ru, but lacks Co quencher. Instrument settings: modulation amplitude = 10 G at 100 kHz; frequency = 9.37 GHz; microwave power = 6.4 mW; and temperature = 10 K.

In a sample containing 20 μM Dps loaded with 12 Fe(II)/Dps, poly(dGdC)$_2$ at a concentration of 1 mM base-pairs, 20 μM noncovalent [Ru(phen) (dppz) (bpy′)]$^{2+}$ and 120 μM [Co(NH$_3$)$_5$Cl]$^{2+}$ in a buffer of 50 mM Tris, pH 7.0, 150 mM NaCl, 5% glycerol, a split nearly isotropic signal at g = 4.3 is observed upon irradiation (Figure 3). Comparison with the chemically oxidized sample indicates that this species corresponds to oxidized ferric iron at the mononuclear ferroxidase site in Dps that was formed after DNA oxidation with the ruthenium photooxidant. DC subtracted spectra in this trial were quantified by double integration over the range of 1400 to 1700 gauss. Consistent trends were seen in two separate trials. In contrast to the full sample (containing poly(dGdC)$_2$ DNA, ferrous iron-loaded Dps, Ru photooxidant, and Co quencher), an 8-fold decreased signal was observed in a

DOI: 10.1021/jacs.6b06507
J. Am. Chem. Soc. 2016, 138, 11290−11298

sample lacking DNA (Minus DNA). An attenuated signal was also observed in an irradiated sample that contained ferrous iron-loaded Dps, poly(dGdC)$_2$, and [Ru(phen) (dppz) (bpy′)]$^{2+}$ but lacked quencher (Light control). Some signal was observed in the light control sample (1.7-fold less than the full sample), even though steady-state room temperature luminescence experiments with mixed-sequence 70-mer duplex DNA containing covalently tethered [Ru(phen) (dppz) (bpy′)]$^{2+}$ indicated that Dps does not quench the ruthenium-(II) excited state.[11] When Apo-Dps is substituted for Dps loaded with ferrous iron, no signal at g = 4.3 is observed, confirming protein-bound iron as the origin of this signal. Importantly, when poly(dAdT)$_2$ is substituted for poly-(dGdC)$_2$, the observed signal is significantly attenuated (3.0-fold), suggesting that guanine radicals play a role in Dps oxidation.

The wide EPR spectrum of the sample containing poly-(dGdC)$_2$ with ferrous iron-loaded Dps from 500 to 4500 gauss shows that the features evident upon irradiation are the g = 4.3 signal previously discussed, a broad signal at lower magnetic fields due to Co^{2+} produced in the flash-quench reaction, and a small signal at g = 2 (Figure S1). The g = 2 signal is likely an organic radical, either guanine radical or tryptophan radical; however, we were unable to obtain reproducible results at g = 2. Despite investigating different temperatures and microwave powers to prevent power saturation, signals at g = 2 were too small for conclusions to be drawn. While the tryptophan radical (W52) has been previously observed in *E. coli* Dps with UV–visible stopped-flow experiments,[15] it is likely that we lack the time resolution to observe this radical with EPR. In Tris buffer, there is a signal at g = 4.3 when a sample of ferrous iron only is mixed with ferricyanide (Figure S2). Therefore, it is important to control for oxidized iron remaining bound to Dps in DNA photooxidation experiments. One approach is to compare samples prepared in a MOPS buffer. In MOPS buffer, no signal is observed when a sample of ferrous iron only is mixed with ferricyanide (Figure S3). However, a small, unsplit signal is apparent at g = 4.3 in a sample of ferrous iron-loaded Dps, poly(dGdC)$_2$ DNA, ruthenium photooxidant and diffusing quencher upon irradiation. While the significantly smaller signals in MOPS buffer makes comparisons between samples (i.e., different DNAs) difficult, this MOPS result suggests that at least some of the free iron in Tris samples remains bound to the protein after oxidation.

Structure and Fe Binding of W52 Dps Mutants. The Dps monomer is composed of a four helix bundle with two helix-turn-helix motifs.[28] The far-UV circular dichroism (CD) spectra of WT Apo-Dps is consistent with this α-helical structure[29] (Figure 4). Comparison of the WT, W52A, and W52Y Dps CD spectra show that overall protein folding is relatively unaffected by these mutations.

Iron binding at the ferroxidase site was also investigated for both mutations. As previously described for WT Dps,[11] the proteins were incubated anaerobically with excess ferrous iron and unbound iron was subsequently removed with size exclusion chromatography. The number of irons bound per Dps dodecamer was then quantified by the formation of [Fe(bpy)$_3$]$^{2+}$ after protein denaturation and addition of reductant and 2,2′-bipyridine. When Dps concentration is measured via the Bradford reagent or calculated ε_{280} values, the Fe(II)/Dps can be quantified. In one trial, the WT protein bound 14.6 ± 0.5 Fe(II)/Dps, whereas the W52A and W52Y mutants bound only 8.6 ± 0.4 and 10.6 ± 0.4 Fe(II)/Dps,

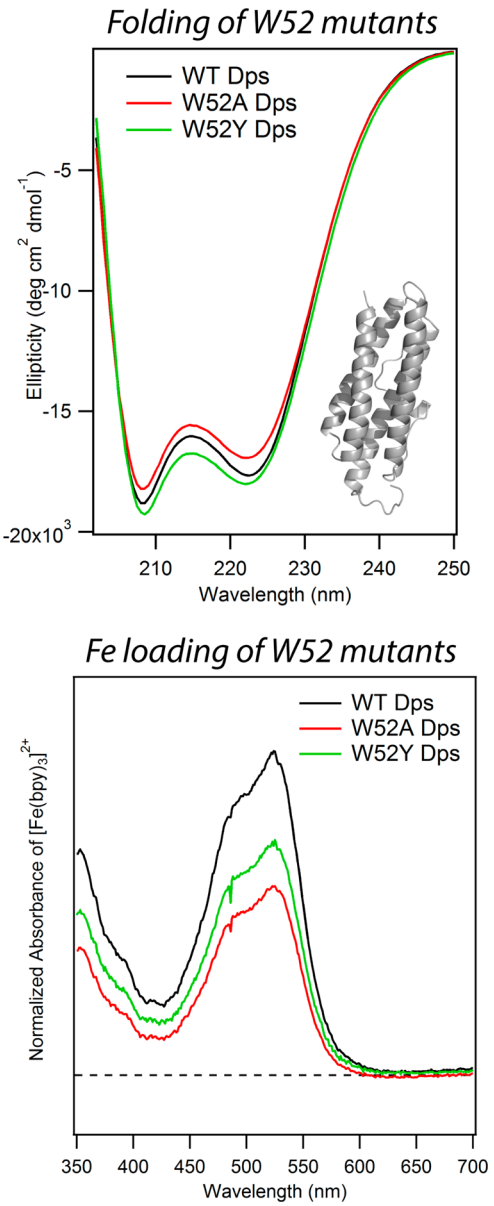

Figure 4. Folding and iron loading of W52 Dps mutants. (Upper) Circular dichroism spectra of wild-type (WT) (black), W52A (red), and W52Y (green) *E. coli* Apo-Dps. Dps monomer depicted in gray, showing α-helical structure (PDB: 1DPS). Protein concentration was 5 μM in a buffer of 50 mM Tris, pH 7.0, 150 mM NaCl. (Lower) Ferrous iron loading of Dps W52 mutants compared to WT *E. coli* protein. Normalized UV–vis spectra of [Fe(bpy)$_3$]$^{2+}$ produced from either WT Dps (black), W52A Dps (red), or W52Y Dps (green). For normalization, the absorbance values were divided by protein concentration. The calculated number of iron atoms per Dps dodecamer is 14.6 ± 0.5 for WT Dps, 8.6 ± 0.4 for W52A, and 10.6 ± 0.4 for W52Y. Protein concentrations were determined as given in the Experimental Section .

respectively. Equivalent results were obtained in other trials. Note that small increases from 12 Fe(II)/Dps in the WT protein are likely due to a minor degree of oxidation due to trace oxygen, allowing for some di-iron site formation. Figure 4 shows the [Fe(bpy)$_3$]$^{2+}$ spectra normalized to protein concentration for WT, W52A, and W52Y Dps. W52A Dps binds iron on the order of 60% of WT, while W52Y is slightly better, binding 70% of the iron of WT Dps. Thus, iron binding

DOI: 10.1021/jacs.6b06507
J. Am. Chem. Soc. 2016, 138, 11290–11298

is somewhat attenuated, but not abrogated, for these mutations. Furthermore, these W52 mutations are not expected to affect the DNA binding of Dps; previous work demonstrated that iron-loaded Dps binds DNA similarly to the Apo-protein.[11] Additionally, we observed the same level of precipitation and DNA condensation with the W52 mutants and WT.

EPR Results Comparing WT Dps with W52 Mutants. The ability of ferrous iron-loaded W52A and W52Y Dps to be oxidized by ferricyanide, a diffusing oxidant, was first explored using EPR spectroscopy. Figure 5A shows oxidation of the W52 mutants compared to WT with excess ferricyanide, with the EPR intensity adjusted for iron loading (i.e., Intensity/(Fe_{W52A}/Fe_{WT})). When the intensity of the EPR signal resulting from ferricyanide oxidation is adjusted for iron loading in this manner, the W52 mutants show similar yields of iron oxidation to WT Dps, with W52Y showing a slightly increased signal relative to WT. This result indicates that oxidation of the mononuclear iron site by a diffusing oxidant is not affected in W52A and W52Y Dps compared to WT.

Next, the X-band EPR spectrum of ferrous iron-loaded WT *E. coli* Dps was compared to W52A and W52Y Dps upon DNA photooxidation using the flash-quench technique. Samples containing ferrous iron-loaded Dps, poly(dGdC)$_2$ DNA, non-covalent [Ru(phen) (dppz) (bpy′)]$^{2+}$ and[$Co(NH_3)_5Cl]^{2+}$ were irradiated for identical lengths of time. The yield of iron oxidation at g = 4.3 was attenuated in the W52 mutants compared to the WT protein, even when adjusted for iron loading (Figure 5B). Overall smaller signals in Figure 5B compared to the WT spectra in Figure 3 are due to a lower modulation amplitude in the former (5 and 10 G, respectively), while the intensity difference between Figure 5, parts A and B, is likely due to a poor kinetic window and inefficieny in irradiation for observing DNA photooxidation. When the DC-subtracted, adjusted spectra are quantified by double integration from 1400 to 1600 gauss, the W52A iron signal is 3.4-fold less than WT, while the W52Y signal is 1.8-fold less than WT. The proficiency in oxidation of the iron sites in these W52 Dps mutants by a chemical oxidant that directly diffuses to the iron site, combined with the deficiency in the yield of iron oxidation upon DNA photooxidation, suggests that W52 could play a role in mediating ET from the iron site to the DNA. As with WT Dps, we do not have the time resolution to observe a tryptophan or tyrosine radical directly using EPR spectroscopy.

It is noteworthy that the EPR spectra of DC samples (i.e., before irradiation) of the W52 mutants show evidence of Co^{2+} formation, whereas the WT protein does not (Figure S4). The cobalt quencher, $[Co(NH_3)_5Cl]^{2+}$, is a low-spin Co^{3+} d^6 species with S = 0. Upon reduction to Co^{2+}, the complex becomes labile, forming $[Co(H_2O)_6]^{2+}$, a high-spin d^7 species with S = 3/2 (EPR-active). Therefore, there may be some direct electron transfer from the ferrous mononuclear iron site to the Co^{3+} quencher to yield EPR-active Co^{2+} in these mutants, perhaps because the ferroxidase site is more solvent-accessible. However, there is very little evidence of ferric iron formation in the DC spectrum of the W52A mutant, and in W52Y, a relatively small percentage of the total amount of iron in the sample is oxidized, allowing ample room for an increase upon irradiation. Thus, the lower yield of iron oxidation that we observe upon DNA photooxidation with the W52 mutants is significant, supporting our EPR results that suggest W52 as an electron transfer intermediate in Dps.

Hydrogen Peroxide Survival Assay. The biological consequence of mutating W52 was also investigated by measuring the survival of *E. coli* upon exposure to hydrogen peroxide for cells containing WT, W52A, or W52Y Dps. The *dps* knockout *E. coli* strain (*dps*::*kan* Δ*recA* Δ*ara*) (ZK2471) was transformed with a pBAD18 plasmid containing either the

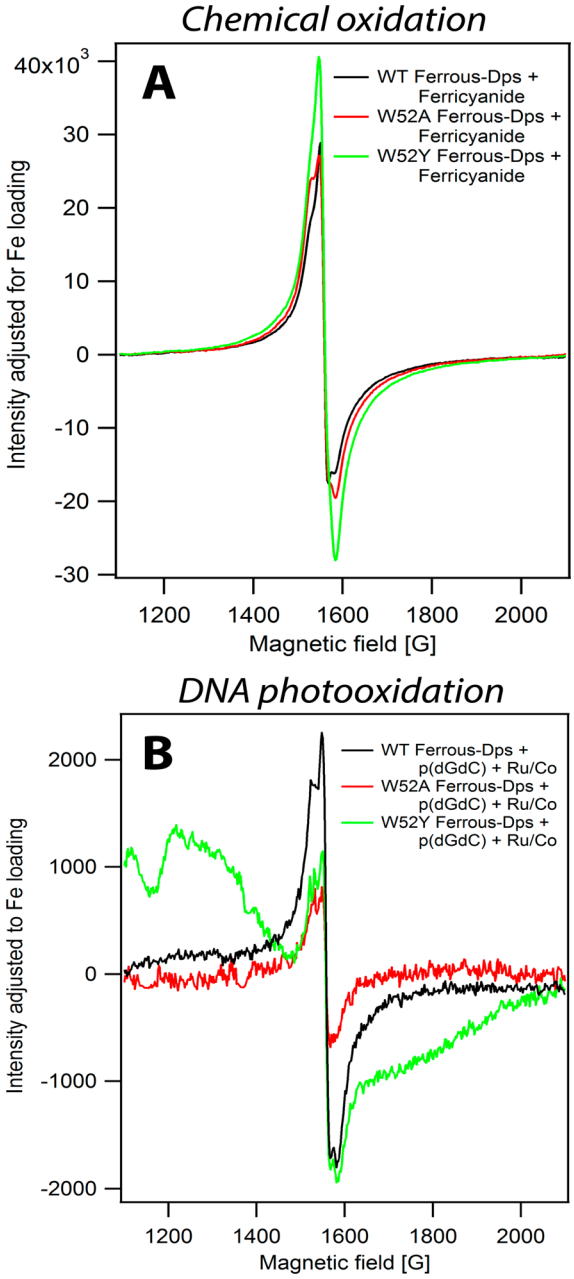

Figure 5. Comparison of chemical oxidation of ferrous iron-loaded Dps with ferricyanide, and oxidation following DNA photooxidation. EPR intensity for the Dps mutants was adjusted to that of the WT protein via dividing by the ratio Fe_{W52}/Fe_{WT}. (A) Oxidation by 2-fold excess ferricyanide: 20 μM Dps (Fe^{2+}/Dps: WT: 13.6 ± 0.2, W52A: 8.8 ± 0.2; W52Y: 11.3 ± 0.1), 480 μM ferricyanide. (B) Comparison of ferrous iron-loaded WT Dps and W52A/Y mutant following DNA photooxidation. All spectra have had an individual unirradiated spectrum subtracted. Concentrations: 20 μM Dps (Fe^{2+}/Dps: WT: 16.0 ± 0.5, W52A: 10.1 ± 0.2; W52Y: 11.5 ± 0.2), 1 mM base-pairs poly(dGdC)$_2$ DNA, 20 μM [Ru(phen) (dppz) (bpy′)]$^{2+}$, 120 μM $[Co(NH_3)_5Cl]^{2+}$. 50 mM Tris, pH 7.0, 150 mM NaCl, 5% glycerol. Modulation amplitude = 10 G in (A) and 5 G in (B) at 100 kHz; frequency = 9.37 GHz; microwave power = 6.4 mW; and temperature = 10 K.

DOI: 10.1021/jacs.6b06507
J. Am. Chem. Soc. 2016, 138, 11290−11298

E. coli WT, W52A, or W52Y *dps* gene under the control of an inducible promoter. In the absence of hydrogen peroxide at the inducer concentrations used in this study, no growth difference was observed between the strains (Figure S5).

Adapted from the method of Martinez and Kolter,[20] cells were grown overnight and diluted into fresh media with the addition of either the inducer (+), L-arabinose, or sterile water (−). Cells were then grown to exponential phase (OD600 = 0.3−0.4) and challenged with 3 or 5 mM hydrogen peroxide. After quenching the reaction with catalase, cells were diluted and plated in multiple droplets to quantify colony forming units (CFU). The results from the 0.2% w/v of L-arabinose inducer at 10 000-fold dilution are shown in Figure 6. Percent survival

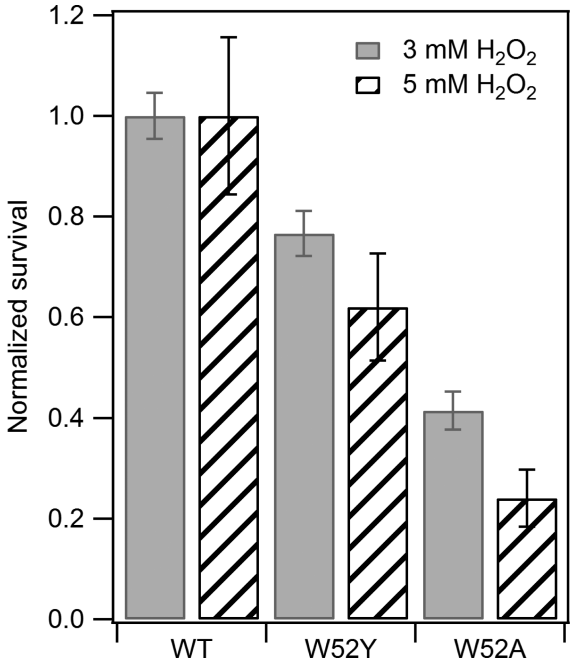

Figure 6. Hydrogen peroxide survival assay comparing *E. coli* with WT, W52Y, or W52A Dps. Dps has been induced with 0.2% w/v L-arabinose and cells treated with either 3 (solid gray bars) or 5 (dashed bars) mM hydrogen peroxide. Percent survival was calculated as the fraction of surviving colonies over the number of CFUs seeded (seeded CFUs calculated by dilution-adjusted OD_{600} readings). Each mutant data set was normalized to the WT survival percentage. The standard error of the mean was calculated by treating each droplet as a data point.

was calculated as the fraction of surviving colonies over the number of seeded CFUs as calculated by dilution-adjusted OD_{600} readings. Each mutant data set was then normalized to the WT survival percentage. The standard error of the mean was calculated by treating each droplet as a data point (n = 16). Raw data are shown in Figure S6. As was previously observed,[20] there is also a clear difference in bacterial survival after treatment with hydrogen peroxide between induced and uninduced cells (Figure S7) demonstrating that Dps is needed for protection.

As is evident in Figure 6, cells containing W52Y Dps survive the hydrogen peroxide challenge more effectively than those with W52A Dps. Additionally, the relative percent survival varies with hydrogen peroxide concentration. Whereas at 3 mM H_2O_2, cells containing W52Y and W52A Dps survive at levels 77% and 41% of WT, respectively, when cells are further challenged by 5 mM hydrogen peroxide, survival drops to 62% of WT for W52Y and 24% for W52A Dps cells. Thus, W52 is an essential player for cells containing Dps to survive this hydrogen peroxide challenge. There is certainly a component of Dps Fe loading proficiency (W52Y and W52A Dps bind iron at approximately 70% and 60%, respectively, of WT, vide supra) in this survival. However, the difference between observed survival and Dps Fe loading, combined with the variation of survival with H_2O_2 concentration shows that an additional component also affects survival; we propose that this factor may be the efficiency of DNA CT. Furthermore, this in vivo trend (WT > W52Y > W52A) parallels what we observe in EPR experiments, where the largest attenuation in the yield of iron oxidation following DNA photooxidation is seen with W52A Dps. The correlation between our EPR and in vivo experiments supports our proposal that survival depends on both Dps Fe loading proficiency and the efficiency of DNA CT.

DISCUSSION

In earlier studies, we have shown biochemically that ferrous iron-loaded *E. coli* Dps can protect DNA from oxidative damage generated using the flash-quench technique.[11] The absence of this protective ability in Apo-Dps and Dps loaded with ferric iron, which both lack available reducing equivalents, suggested that ferrous-iron loaded Dps protects DNA by becoming oxidized via DNA CT to fill guanine radical holes. Here using EPR, we show directly the oxidation of WT ferrous iron-loaded *E. coli* Dps following DNA photooxidation generated by the flash-quench technique. Because Dps is loaded with one ferrous iron per ferroxidase site, this oxidation is evidenced by the appearance of mononuclear ferric iron species of low symmetry at an apparent g-value of 4.3. This signal is absent in controls without DNA and is attenuated in the irradiated control that lacks the diffusing quencher necessary for oxidation by flash-quench.

The results described here furthermore support the idea that guanine radicals facilitate Dps oxidation. When poly(dGdC)$_2$ is substituted with poly(dAdT)$_2$, the yield of Dps oxidation is decreased significantly. A similar dependence on guanine radicals was observed in the oxidation of the 4Fe4S cluster of the base excision repair protein MutY following DNA photooxidation by flash-quench.[12b] More efficient protein oxidation by guanine radicals is likely a kinetic effect. Back electron transfer processes generally decrease the observed yield of oxidized protein using the flash-quench technique. Adenine radicals would be expected to have short lifetimes compared to the neutral guanine radical, which persists for milliseconds.[12a] Thus, as was described for MutY,[12b] it appears likely that guanine radical formation allows more time for the oxidation of Dps by better competing with rapid back electron transfer to the intercalated ruthenium photooxidant, resulting in higher yields of Dps oxidation with guanine radical as an intermediate. Additionally, poorly stacked ATAT tracts do not conduct charge efficiently;[30] this poor CT may also be a factor in the lower yield of protein oxidation with poly(dAdT)$_2$ DNA. Generally, the more favorable oxidation of Dps by guanine radicals also supports a sequential process, using DNA-mediated CT, where after guanine radicals are produced, Dps is oxidized to fill guanine radical holes.

Can we also obtain information concerning the path for electron transfer? In 12-mer Dps proteins, there is a conserved tryptophan residue in close proximity to the ferroxidase site (W52 in the *E. coli* protein), whereas 24-mer ferritins contain a

DOI: 10.1021/jacs.6b06507
J. Am. Chem. Soc. 2016, 138, 11290−11298

conserved tyrosine residue. In both cases, this aromatic residue has been proposed to act as a molecular capacitor, providing an extra electron during iron oxidation in order to prevent formation of oxygen radicals.[15,16] The location of the conserved tryptophan residue in Dps proteins between the ferroxidase site and protein surface suggests a possible role for the tryptophan as an electron transfer hopping intermediate in the DNA-mediated oxidation of the iron site.

Here we use site-directed mutagenesis, creating W52A and W52Y *E. coli* Dps, to investigate this possibility. While overall protein folding seems unaffected by these mutations, iron binding is somewhat attenuated. When adjusted for iron loading, the yield of Dps oxidation by a diffusing oxidant, ferricyanide, is not attenuated by these W52 mutations. However, even adjusted for iron loading, the level of iron oxidation observed in EPR experiments upon DNA photo-oxidation for both W52A and W52Y Dps is significantly reduced with respect to the WT protein, with a more significant attenuation for W52A Dps. These observations suggest that W52 may play a role in mediating CT from the iron site to DNA. Because (i) the intercalating ruthenium photooxidant is a one-electron oxidant, and (ii) the mononuclear iron site has a much lower redox potential (as indicated by its oxidation by ferricyanide, 0.43 V versus NHE[31]) than tryptophan or tyrosine, making it the thermodynamic sink, the deficiency in iron oxidation for these mutants suggests a role for W52 as an electron transfer hopping intermediate rather than as a molecular capacitor.

While we may understand how the W52A mutation might inhibit CT by deleting the aromatic residue that mediates electronic coupling, why might substitution of tryptophan with an aromatic tyrosine residue have such an effect? Work by Gray and co-workers has revealed that precise tuning of the reduction potential of hopping intermediates is essential for function.[32,33] With tyrosine, the reduction potential can be modulated by adjacent basic amino acids such as His, Asp, or Glu that can hydrogen bond with the OH group of tyrosine.[33] In *E. coli* Dps, no basic residues are in the vicinity of Y52 except for the ferroxidase site ligands, which are presumably coordinating iron. Therefore, the Dps protein environment may support a tryptophan radical but not be as amenable to a tyrosine radical at the reduction potentials necessary for a hopping intermediate.

We also probed the role of *E. coli* W52 Dps in cells through tests of cell survival under stress of hydrogen peroxide. Bacteria containing WT Dps are best able to survive this oxidative stress. Whereas there is some attenuation in survival seen for cells containing W52Y Dps, cells containing W52A Dps show significantly diminished survival. It appears then that the conserved tryptophan residue in close proximity to the ferroxidase site in Dps proteins is important for bacteria containing Dps to survive under conditions of oxidative stress. This survival likely depends on both the Dps iron loading proficiency and an additional factor that we propose to be the ability of the Dps protein to facilitate efficient DNA CT. Moreover, the survival trend that we observe in bacteria under oxidative stress mirrors the Dps photooxidation proficiency observed in EPR experiments. Thus, some of this in vivo effect may be due to inhibition of the DNA-mediated oxidation of Dps upon mutation of W52. Perhaps Y52 can still act as a molecular capacitor inside cells, preventing ROS formation in the hydrogen peroxide oxidation of mononuclear iron sites, but it is less able to act as a hopping intermediate because of nonoptimal protein environment. A52 would be unable to fulfill either function in Dps proteins, and it is interesting that this mutant shows the most deficiency in survival. Overall, mutations to W52 in *E. coli* Dps impair the ability of the bacteria to survive oxidative stress, and we hypothesize that a component of this deficiency derives from a decreased ability to mediate ET from the iron site of Dps to the DNA.

CONCLUSIONS

Dps proteins are involved in the survival and virulence of pathogenic bacteria in response to oxidative stress generated by the host immune system and antibiotics.[34−41] Elucidating the mechanism of Dps protection of the genomes of pathogenic bacteria may inform the development of new antibiotic therapies. A long-distance Dps protection mechanism via DNA CT could be an efficient strategy for maintaining the integrity of genomic DNA. In this work, we further explore the DNA-mediated oxidation of the bacterial ferritin Dps. We use EPR to characterize spectroscopically the oxidation of ferrous iron-loaded Dps following DNA photooxidation via the flash-quench technique. We find that guanine sequences facilitate Dps oxidation. Furthermore, we explore possible ET intermediates within the Dps protein fold in the DNA-mediated oxidation, focusing on a conserved tryptophan residue in close proximity to the ferroxidase site of Dps proteins. In EPR experiments, the yield of Dps oxidation upon DNA photooxidation is significantly attenuated for W52A Dps compared to the WT protein. This effect is reflected in vivo in *E. coli* survival in response to hydrogen peroxide, suggesting that some of this in vivo survival decrease could be due to inhibition of the DNA-mediated oxidation of Dps upon mutation of W52.

Thus, we have moved toward understanding the role that DNA CT may play with Dps proteins inside cells. Interestingly, Dps seems to act as a checkpoint during oxidative stress to delay the initiation of DNA replication in *E. coli* until oxidative DNA damage has been repaired.[42] This interplay of DNA protection by Dps with repair and replication may be considered in the context of long-range signaling through DNA CT.[6] Certainly the function of Dps proteins in the long-range DNA-mediated protection of the genome from oxidative assault requires further consideration as targets in the treatment of pathogenic bacteria.

ASSOCIATED CONTENT

Supporting Information

The Supporting Information is available free of charge on the ACS Publications website at DOI: 10.1021/jacs.6b06507.

Primer sequences, detailed Dps overexpression and purification protocol, and Figures S1−S7 (PDF)

AUTHOR INFORMATION

Corresponding Author

*jkbarton@caltech.edu

Notes

The authors declare no competing financial interest.

ACKNOWLEDGMENTS

We are grateful for the financial support of the National Institutes of Health and the Moore Foundation. A.R.A. was supported by the National Institute on Aging of the NIH on a predoctoral NRSA (F31AG040954), and A.Z. through an NSF

DOI: 10.1021/jacs.6b06507
J. Am. Chem. Soc. 2016, 138, 11290−11298

fellowship. We thank Dr. Angelo Di Bilio for his assistance with EPR instrumentation. We also thank Stephanie Gu for her contributions to the hydrogen peroxide survival assay during her Caltech SURF experience.

REFERENCES

(1) Chiancone, E.; Ceci, P. *Biochim. Biophys. Acta, Gen. Subj.* **2010**, *1800*, 798−805.
(2) Zhao, G.; Ceci, P.; Ilari, A.; Giangiacomo, L.; Laue, T. M.; Chiancone, E.; Chasteen, N. D. *J. Biol. Chem.* **2002**, *277*, 27689−27696.
(3) Ceci, P.; Cellai, S.; Falvo, E.; Rivetti, C.; Rossi, G. L.; Chiancone, E. *Nucleic Acids Res.* **2004**, *32*, 5935−5944.
(4) Altuvia, S.; Almiron, M.; Huisman, G.; Kolter, R.; Storz, G. *Mol. Microbiol.* **1994**, *13*, 265−272.
(5) Wolf, S. G.; Frenkiel, D.; Arad, T.; Finkel, S. E.; Kolter, R.; Minsky, A. *Nature* **1999**, *400*, 83−85.
(6) (a) Grodick, M. A.; Muren, N. B.; Barton, J. K. *Biochemistry* **2015**, *54*, 962−973. (b) Arnold, A. R.; Grodick, M. A.; Barton, J. K. *Cell Chemical Biology* **2016**, *23*, 183−197.
(7) (a) Boal, A. K.; Genereux, J. C.; Sontz, P. A.; Gralnick, J. A.; Newman, D. K.; Barton, J. K. *Proc. Natl. Acad. Sci. U. S. A.* **2009**, *106*, 15237−15242. (b) Grodick, M. A.; Segal, H. M.; Zwang, T. J.; Barton, J. K. *J. Am. Chem. Soc.* **2014**, *136*, 6470−6478.
(8) Saito, I.; Nakamura, T.; Nakatani, K.; Yoshioka, Y.; Yamaguchi, K.; Sugiyama, H. *J. Am. Chem. Soc.* **1998**, *120*, 12686−12687.
(9) (a) Hall, D. B.; Holmlin, R. E.; Barton, J. K. *Nature* **1996**, *382*, 731−735. (b) Arkin, M. R.; Stemp, E. D. A.; Pulver, S. C.; Barton, J. K. *Chem. Biol.* **1997**, *4*, 389−400.
(10) Slinker, J. D.; Muren, N. B.; Renfrew, S. E.; Barton, J. K. *Nat. Chem.* **2011**, *3*, 230−235.
(11) Arnold, A. R.; Barton, J. K. *J. Am. Chem. Soc.* **2013**, *135*, 15726−15729.
(12) (a) Stemp, E. D. A.; Arkin, M. R.; Barton, J. K. *J. Am. Chem. Soc.* **1997**, *119*, 2921−2925. (b) Yavin, E.; Boal, A. K.; Stemp, E. D. A.; Boon, E. M.; Livingston, A. L.; O'Shea, V. L.; David, S. S.; Barton, J. K. *Proc. Natl. Acad. Sci. U. S. A.* **2005**, *102*, 3546−3551.
(13) Ren, B.; Tibbelin, G.; Kajino, T.; Asami, O.; Ladenstein, R. *J. Mol. Biol.* **2003**, *329*, 467−477.
(14) Winkler, J. R.; Gray, H. B. *Chem. Rev.* **2014**, *114*, 3369−3380.
(15) Bellapadrona, G.; Ardini, M.; Ceci, P.; Stefanini, S.; Chiancone, E. *Free Radical Biol. Med.* **2010**, *48*, 292−297.
(16) The reduction of hydrogen peroxide to water is a two electron process, but this study was conducted under iron loading conditions that preclude formation of the di-iron site that would provide two electrons. Thus, these aromatic residues may provide the extra electron that would otherwise be abstracted from DNA, resulting in oxidative damage.
(17) (a) Ebrahimi, K. H.; Hagedoorn, P.-L.; Hagen, W. R. *ChemBioChem* **2013**, *14*, 1123−1133. (b) Bou-Abdallah, F.; Yang, H.; Awomolo, A.; Cooper, B.; Woodhall, M. R.; Andrews, S. C.; Chasteen, N. D. *Biochemistry* **2014**, *53*, 483−495.
(18) Sovenyhazy, K. M.; Bordelon, J. A.; Petty, J. T. *Nucleic Acids Res.* **2003**, *31*, 2561−2569.
(19) Anderson, P. A.; Deacon, G. B.; Haarmann, K. H.; Keene, F. R.; Meyer, T. J.; Reitsma, D. A.; Skelton, B. W.; Strouse, G. F.; Thomas, N. C.; Treadway, J. A.; White, A. H. *Inorg. Chem.* **1995**, *34*, 6145−6157.
(20) Martinez, A.; Kolter, R. *J. Bacteriol.* **1998**, *179*, 5188−5194.
(21) Su, M.; Cavallo, S.; Stefanini, S.; Chiancone, E.; Chasteen, N. D. *Biochemistry* **2005**, *44*, 5572−5578.
(22) A bridging oxygen atom seems to be required to form the di-iron site.
(23) Schwartz, J. K.; Liu, X. S.; Tosha, T.; Diebold, A.; Theil, E. C.; Solomon, E. I. *Biochemistry* **2010**, *49*, 10516−10525.
(24) Bou-Abdallah, F.; Chasteen, N. D. *JBIC, J. Biol. Inorg. Chem.* **2007**, *13*, 15−24.
(25) Gibson, J. F. *ESR and NMR of Paramagnetic Species in Biological and Related Systems*; Bertini, I., Drago, R. S., Eds.; Springer: Netherlands, 1979; pp 225−253.
(26) Sun, S.; Chasteen, N. D. *Biochemistry* **1994**, *33*, 15095−15102.
(27) Ardini, M.; Fiorillo, A.; Fittipaldi, M.; Stefanini, S.; Gatteschi, D.; Ilari, A.; Chiancone, E. *Biochim. Biophys. Acta, Gen. Subj.* **2013**, *1830*, 3745−3755.
(28) Grant, R. A.; Filman, D. J.; Finkel, S. E.; Kolter, R.; Hogle, J. M. *Nat. Struct. Biol.* **1998**, *5*, 294−303.
(29) Kelly, S. M.; Jess, T. J.; Price, N. C. *Biochim. Biophys. Acta, Proteins Proteomics* **2005**, *1751*, 119−139.
(30) O'Neill, M. A.; Barton, J. K. *J. Am. Chem. Soc.* **2004**, *126*, 11471−11483.
(31) Dutton, P. L. *Methods Enzymol.* **1978**, *54*, 411−435.
(32) Shih, C.; Museth, A. K.; Abrahamsson, M.; Blanco-Rodriguez, A. M.; Di Bilio, A. J.; Sudhamsu, J.; Crane, B. R.; Ronayne, K. L.; Towrie, M.; Vlček, A., Jr.; Richards, J. H.; Winkler, J. R.; Gray, H. B. *Science* **2008**, *320*, 1760−1762.
(33) Warren, J. J.; Winkler, J. R.; Gray, H. B. *FEBS Lett.* **2012**, *586*, 596−602.
(34) Sund, C. J.; Rocha, E. R.; Tzinabos, A. O.; Wells, W. G.; Gee, J. M.; Reott, M. A.; O'Rourke, D. P.; Smith, C. J. *Mol. Microbiol.* **2008**, *67*, 129−142.
(35) Li, X.; Pal, U.; Ramamoorthi, N.; Liu, X.; Desrosiers, D. C.; Eggers, C. H.; Anderson, J. F.; Radolf, J. D.; Fikrig, E. *Mol. Microbiol.* **2007**, *63*, 694−710.
(36) Satin, B.; Del Giudice, G.; Bianca, V. D.; Dusi, S.; Laudanna, C.; Tonello, F.; Kelleher, D.; Rappuoli, R.; Montecucco, C.; Rossi, F. *J. Exp. Med.* **2000**, *191*, 1467−1476.
(37) Halsey, T. A.; Vazquez-Torres, A.; Gravdahl, D. J.; Fang, F. C.; Libby, S. J. *Infect. Immun.* **2004**, *72*, 1155−1158.
(38) Pang, B.; Hong, W.; Kock, N. D.; Swords, W. E. *Front. Cell. Infect. Microbiol.* **2012**, *2*, Article 58.
(39) Theoret, J. R.; Cooper, K. K.; Zekarias, B.; Roland, K. L.; Law, B. F.; Curtiss, R., 3rd; Joens, L. A. *Clin. Vaccine Immunol.* **2012**, *19*, 1426−1431.
(40) Olsen, K. N.; Larsen, M. H.; Gahan, C. G. M.; Kallipolitis, B.; Wolf, X. A.; Rea, R.; Hill, C.; Ingmer, H. *Microbiology* **2005**, *151*, 925−933.
(41) Calhoun, L. M.; Kwon, Y. M. *Int. J. Antimicrob. Agents* **2011**, *37*, 261−265.
(42) Chodavarapu, S.; Gomez, R.; Vicente, M.; Kaguni, J. M. *Mol. Microbiol.* **2008**, *67*, 1331−1346.

DOI: 10.1021/jacs.6b06507
J. Am. Chem. Soc. 2016, 138, 11290−11298